FIELD IMPLEMENTATION and TRIAL of COORDINATED CONTROL of WIND FARMS

Tanvir Ahmad, Olivier Coupiac, Arthur Petit, Sophie Guignard, Nicolas Girard, Behzad Kazemtabrizi and Peter Matthews

***Abstract*—This paper demonstrates, with live field experiment, the potential of increasing wind farm production through minimising wake effects by curtailing upstream wind turbines. Two 2MW turbines from the SMV (Le Sole de Moulin Vieux) wind farm are used for this purpose. The farm is equipped with state of the art LiDARs (Light Detection And Ranging) for measuring wind characteristics, up to a frequency of 1Hz. Simulations are performed using WindPRO for wake effects prediction. Optimised curtailment strategies are simulated for finding optimum curtailment settings of the upstream turbine. Results based on real time data are compared with simulated results. It is found that simulations are mostly in good agreement with field results, with a maximum difference of 1.5%. Analysis shows that a gain of up to 11.5% is possible in downstream turbine production, using a hard curtailment strategy by reducing power of the upstream turbine by about 17%. In this experiment, the combined production of the two turbines decreased with the hard curtailment strategy, indicating that the upstream turbine must be optimally curtailed for avoiding any production loss. To the best knowledge of the authors, this is the first practical implementation of LiDAR based coordinated control strategies in an operating wind farm.**

***Index Terms*—Coordinated control of wind farms, wind farm power production maximisation, wind farm control and optimisation, wake mitigation, LiDAR based wind farm control**

I. Introduction

Wind turbines are installed together in wind farms mainly to get advantages of economies of scale. Wind farms reduce civil engineering, grid connection and operation & maintenance costs. Other than economies of scale, factors such as navigational constraints also lead to closely spaced wind turbine in wind farms, such as the Lillgrund wind farm [1]. Though creating wind farms has major benefits, installing turbines in clusters creates aerodynamic interactions, namely wake effects, producing negative impact on farm production. Wake losses can reach as high as 60% in wind farms [1]. Wake effects also increase fatigue loading inside the wind farm. Hence, it is always desirable to mitigate and control wake effects.

This paper presents innovative wind farm coordinated control strategies that reduce wake effects inside the farm. Curtailing upstream turbines by using coefficient of power (C_P) or deflecting the wakes away from downstream turbines using yaw-offsets, can produce a positive impact on downstream turbines' production. The current state of the art control is based on greedy approach, as each turbine only maximises its own production neglecting the wake impact on downstream turbines. Using a coordinated control, the turbine optimises its contribution to the whole farm production along with minimising the wake impact on downstream turbines. This wake minimisation enables the downstream turbine to have a greater production.

Coordinated control of wind farms has recently been an active area of research. A detailed literature review of coordinated control studies is presented in section II. All of the previous studies regarding coordinated control are based either on simulations or scaled wind farms in wind tunnel experiments. There is a lack of field testing for evaluating coordinated control strategies. One major reason for this is the stochastic nature of the wind. There can be great variations in wind speed and direction over a short span of time. This stochastic nature of wind makes it hard to validate the experimental results with the field results. Uncertainties and errors in SCADA data, introduced by nacelle anemometer; especially in wake situations and met mast, adds to the problem.

With the introduction of modern LiDARs, it is now possible to determine the actual wind characteristics in a wind farm [2], [3]. LiDARs can provide information about wind conditions before it reaches the turbines. This information can be used for optimising farm production. In addition to the stochastic nature of the wind, major barriers to the implementation of wind farm coordinated control are the lack of sufficiently fast real-time optimisation and wake modelling methods, and the effective use of LiDAR systems [3]. This paper addresses all these issues by detailing implementation and investigations of C_P-based coordinated control strategies using LiDARs.

A setup of two operating wind turbines in the SMV is used for evaluating the benefits of C_P based coordinated control. The wind farm and turbines are equipped with state of the art LiDARs. The wake assessment methodology detailed in [4] is used for developing a two-step hard curtailment strategy. This hard strategy can curtail the upstream turbine by a maximum of 20% in full or near-full wake conditions on the downstream turbines, in certain wind speeds. Simulations are performed using WindPRO [5] for hard curtailment strategy while optimised control strategy is simulated using TI-JM (Turbulence Intensity based Jensen Model) [4].

The aim of this experiment is to assess the impact of curtailment of an upstream on the downstream turbine and not increasing the combined power production. Hence, a decrease in combined production was expected because of the high curtailment.

This paper is organised as follows. First previous studies of wind farm control are reviewed in section II. Details of the

Tanvir Ahmad is a PhD student and is supervised by Peter Matthews and Behzad Kazemtabrizi at Durham University, UK

Olivier Coupiac, Arthur Petit, Sophie Guignard and Nicolas Girard are from Maïa Eolis (now Engie Green), France

experimental setup are provided in section III. This is followed by the methodology and details of the hard curtailment strategy in section IV. Filtering and availability of data from different sources is detailed in section V. A brief overview of the optimised control strategy and TI-JM is provided in section VI. A short introduction of WindPRO is given in section VII. Analysis based on simulated results are presented in section VIII. The real-time results and analysis are presented in section IX, with conclusions in section X.

II. Literature Review

Wind farm coordinated control and optimisation has been an ongoing research area for the last three decades, as it can improve farm efficiency without any additional material costs. This section reviews previous wind farm coordinated control studies.

Works in [2], [6], [7] use simulations based on artificial wind farms for exploiting benefits of global control of wind farms. The patents [8]–[10] discuss different methods for improving efficiency of wind farms using coordinated control strategies. A complex wake flow model SOWFA (Simulator for Offshore Wind Farm Analysis) is used in [11]–[13] for analysing different curtailment strategies. Simulations with field data using a CFD (Computational Fluid Dynamics) based wind deficit model in [14] optimise wind farm production and loads. Wind tunnel experiments in [8], [15] use axial induction factor for evaluating different control strategies. Wind tunnel experiments and simulations based on data obtained from ECN (Energy Research Centre of the Netherlands) test wind farm in [16]–[21] confirm that if properly implemented, wind farm coordinated control can increase wind farm efficiency and can also decrease fatigue loading on the turbines.

The research presented in [4] has extended the standard Jensen wake model to include turbulence aspects in the TI-JM. By using heuristic optimisation techniques, the TI-JM is able to be used to identify optimal coordinated control strategies based on data from one offshore and two onshore wind farms in [4], [22]. These studies [4], [22] conclude that coordinated control can be beneficial for wind farms in certain wind conditions.

These previous studies are helpful in understanding the impact of curtailment strategies on downstream turbines. What lacks is the implementation and analyses of coordinated control strategies in live operating conditions. This paper fills this gap by applying curtailment strategies in an operating wind farm using LiDARs as discussed in the next section.

III. Experimental Setup

The purpose of this experiment is to implement and analyse C_P-based coordinated control strategies. This experiment started in November 2015 and ended in April 2016 at the SMV wind farm. Details of this field experiment are provided as follows.

A. Le Sole de Moulin Vieux (SMV) wind farm

The SMV wind farm is owned by Maïa Eolis (now Engie Green) and is located in the north of France. The farm consists seven Senvion REpower MM82 2050kW wind turbines [23], installed in a one-dimensional array. Turbines are labelled as SMV1 - SMV7 from north to south as shown in Figure 1. An 80 meters-high lattice met mast with ultrasonic anemometers at 80, 60, 40 and 20m height, is located 1km east of SMV2 and 1.6km north-east of SMV6 as shown in Figure 1. This met mast provides free-stream wind information.

The spacing between the turbines varies between $3.7D$ and $4.3D$. Prevailing wind direction is from south and south-west. The terrain is rough with grass or vegetation. There are woods to the south of the farm as can be seen in Figure 1. The trees are about 15m high and are located at a distance of 100m (less than $1.5D$) from the wind farm. This influences atmospheric stability and results in high turbulence intensity in the wind farm. The farm also suffers from diurnal and seasonal variations in wind conditions [24].

WindPRO suggests free-stream turbulence intensity of 15% for this wind farm clearly exhibiting the roughness on site [5]. This high surface roughness and turbulence intensity result in quick wake recovery. The surrounding wind flow quickly diffuses the momentum loss created by the wakes, resulting in an increased turbulence intensity. This wake added turbulence intensity changes wind characteristics abruptly in the farm.

The experiment focuses on two turbines: SMV5 and SMV6. These two turbines are chosen because of the close spacing ($3.7D$) and prevailing wind direction in the farm. SMV6 is upstream and acts as the wake producing turbine hence curtailment is applied on this turbine. SMV6 is equipped with nacelle mounted Orion 5-beam LiDAR, facing the free-stream wind. A Wind Iris LiDAR is mounted on top of SMV5. A ground based LiDAR, Windcube V1 type has been installed between turbines SMV2 and SMV3. This LiDAR measures wind speed at heights between 40m and 200m with 1Hz frequency. A scanning LiDAR is also installed at 1.2km to the east of the wind farm, as shown in Figure 1. The scanning LiDAR is programmed to carry out three horizontal scans and one vertical scan. This allows hub height measurements of SMV6 in wake situations for SMV5. Full details of the field setup are given in [25].

IV. Methodology

SMV is a one-dimensional array of turbines. When the free-stream wind flows from the east or west, there are no wake effects. However, when the wind flows from the south or north, then the farm production is affected by wake effects. SCADA data from 2011–2014 was used in assessing wake effects in this wind farm in [4]. It was observed that wakes can significantly impact farm production in the direction sector $180^\circ \pm 40^\circ$ and $0^\circ \pm 40^\circ$. Details of this wake assessment methodology and data filtering can be found in [4].

The experiment in this paper used SMV6 and SMV5. Historical wake assessment shows that the wakes from SMV6 can incur significant effects on SMV5 production in the direction sector $200^\circ \pm 20^\circ$ as shown in Figure 2. WindPRO predicts 26% wake losses annually in SMV5 production, caused by SMV6 wakes (normal uncurtailed operation), in this wind direction sector. Hence, this is the chosen direction sector

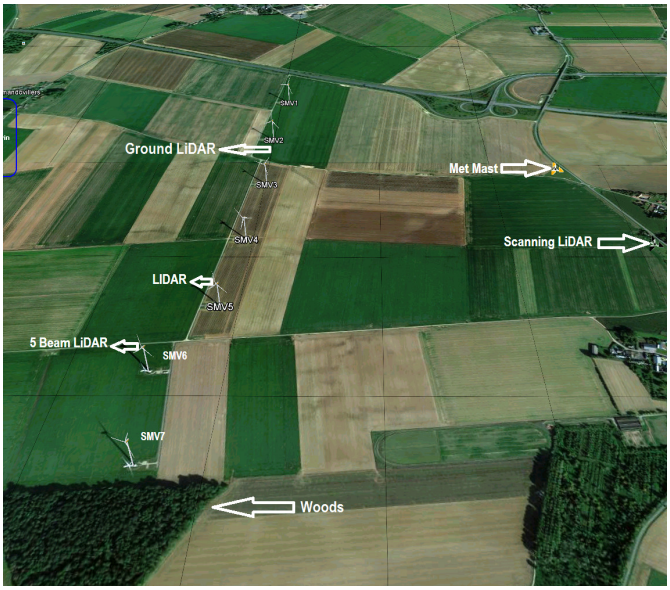

Fig. 1: SMV layout and surrounding with positions of met mast and LiDARs [26]

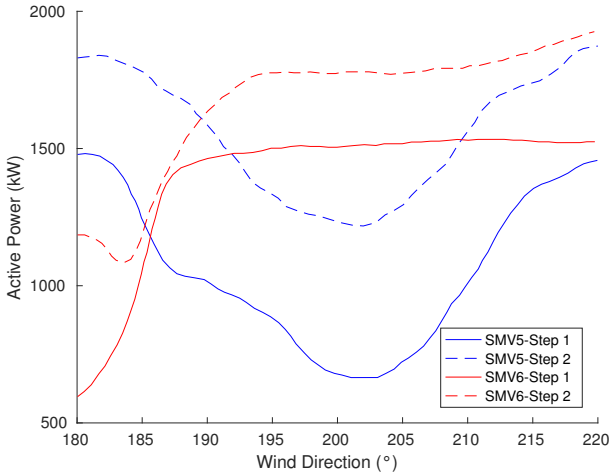

Fig. 2: Wake effects on SMV5 and SMV6 production in $180° - 220°$ during uncurtailed operation.

for this experiment. Figure 2 illustrates the adverse impact the SMV6 wake has on SMV5 production during normal operation. Using the power production of SMV7 as a reference for available wind resource, the production of SMV5 and SMV6 are shown in two different steps. Step 1 represents the lower wind resource availability (SMV7 producing less than 1500kW) and Step 2 represents the higher wind resource availability (SMV7 producing more than 1600kW). From Figure 2, the impact of SMV6 wake on SMV5 can be clearly seen: SMV5 production dips as the wind direction moves the wake from SMV6 fully on to SMV5, with maximal effect at 202°. Similarly, the impact of SMV7 can also be seen on SMV6 production in the region 180°–185°.

A. Hard Curtailment Strategy

A two step C_P-based curtailment strategy, easily implementable on SMV6, was adopted. The strategy is aimed at curtailing SMV6 power to a maximum of 20% in two steps in the selected direction sector as given in Table I. SMV7 production is used as the reference as it is unaffected by wakes when wind flows in the chosen sector. In the first step when SMV7 power is between 1200kW and 1500kW and SMV6 power is above 1200kW then SMV6 is curtailed to 1200kW. In the second step if SMV7 power is between 1600kW and 1900kW and SMV6 power is above 1600kW then SMV6 is curtailed to 1600kW. This curtailment strategy is referred to as hard curtailment strategy due to the hard curtailment limits applied by the wind turbine controller.

TABLE I: Two steps hard curtailment strategy

if 180° ≤ Wind Direction ≤ 220°		
Step 1:	if	1200kW < SMV7 ≤ 1500kW
	then	curtail SMV6 to 1200kW
Step 2:	if	1600kW < SMV7 ≤ 1900kW
	then	curtail SMV6 to 1600kW

When appropriate wind conditions occurred (wind direction and speed), a technician manually curtailed SMV6 accordingly. The wind-rose in Figure 3 shows the wind conditions when SMV6 was actually curtailed as per Table I. The power curve based on this hard curtailment strategy is presented in Figure 4. It can be seen in Figure 4 that SMV6 is curtailed only when the wind speed is above 10m/s.

The Senvion MM82 2050 controller is configured to follow the manufacturer standard power curve by default i.e. the greedy control [23]. This standard power curve is presented in Figure 4. For optimised control, the turbine must follow an optimised power curve for each direction bin. This requires fast processing and efficient control strategies as will be discussed in section VI. It was not possible to implement the optimised power curve during this experiment due to technical limitations [25]. Hence the optimised strategy was only used in simulations for identifying the optimal curtailment settings.

The experiment in this paper is based on curtailment of SMV6 with the wind coming from south and south-west. This takes SMV7 out of analyses as SMV7 is unaffected when SMV6 is curtailed. Hence from this point onwards the wind farm means turbines SMV1 to SMV6.

V. Data and Filtering

During this experiment, data from different sources (metmast, SCADA, LiDAR, and MERRA [27]) were recorded. The availability of data from these sources is shown in Figure 5. The curtailment periods are also given in Figure 5, which represents a total of 19 hours, corresponding to more than 200 data points. To ensure reasonable statistical analysis, it was found that for this data should be placed in bin sizes (resolutions) of 1m/s for wind speed and $\pm 5°$ (i.e. 10° resolution) for wind direction. Wake effects can be assumed to remain the same in these bins, hence averages of the variables under observation are taken in the designated bins. The filtering criteria was set to have at least 10 valid data

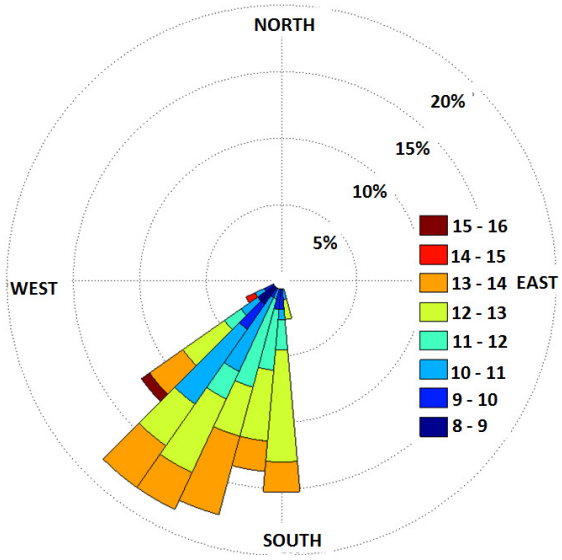

Fig. 3: Wind-rose for the periods when SMV6 was curtailed with the hard strategy

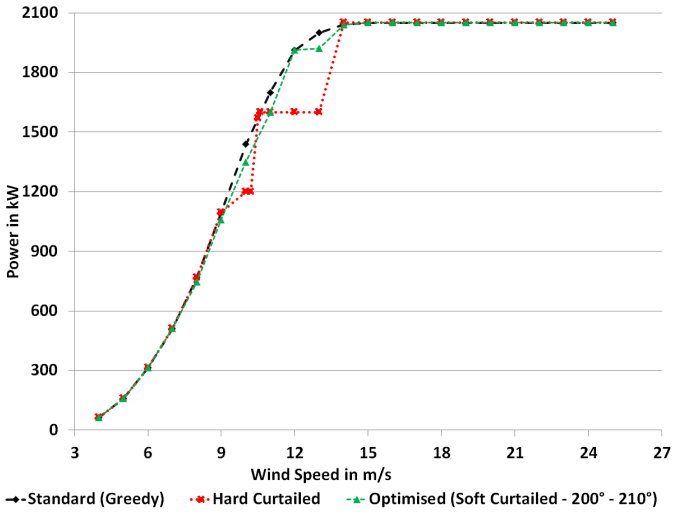

Fig. 4: Comparison of SMV6 standard, hard-curtailed and optimised power curve

points in a given directional and speed bin. Wind conditions with less than 10 data points per bin were not considered for analysis.

Figure 5 also shows atmospheric stability in the wind farm. It can be seen that atmosphere is mostly unstable as discussed in section III-A. This affects the wind conditions inside the wakes and brings abrupt changes in wind direction and speed as discussed in section III-A.

Another important issue was the difference in wind directions, reported by different sources. Instantaneous wind directions can differ from a measuring device placement to another because of wind turbulence. Nevertheless, offsets are mostly due to calibration errors. To avoid any directional discrepancy in analyses, LiDAR Windcube data at a height of 80m was corrected by analysing directions of wakes and then used as a reference. Unlike nacelle mounted instruments,

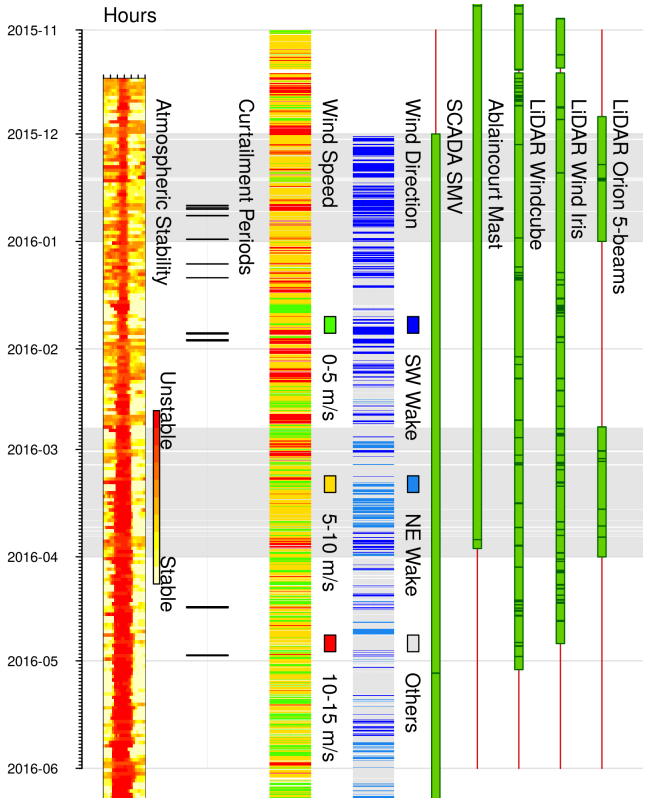

Fig. 5: Data Availability for the experiment from different sources

this LiDAR's wind direction is independent of nacelle position and wake effects do not interfere in directions of interest. Indeed, the measurement of LiDAR wind direction is heavily perturbed in under inhomogeneous wind flow (complex terrain and wake conditions). Finally, directional offsets using this reference were applied to all the devices i.e. LiDARs, turbines and met mast.

VI. Optimised Control

A computationally efficient and optimised control strategy for real-time on-line coordinated control is presented in [4], [22]. The optimised strategy uses the TI-JM for mean production estimation in the farm. The TI-JM estimates wind deficit inside the farm considering deep array effect and wake added turbulence intensity. PSO (Particle Swarm Optimisation) is used for optimising the farm production using C_P-based coordinated control strategies [4], [22].

The optimised strategy curtails SMV6 in such a way that the loss in production is always compensated by gain in SMV5 production. If no level of curtailment results in any increase in the combined (SMV5 + SMV6) production, then the SMV6 follows the standard power curve. The optimised power curve for full wake conditions in the wind direction 200°–210° is presented in Figure 4. This power curve suggests a very small change in the standard power curve from 8–14 m/s. The maximum reduction in SMV6 power is only 4% as compared to the 20% reduction in the hard curtailment strategy. The optimised curtailment requires the power to be

controlled precisely depending on wind speed and direction. This means that each directional bin has its own optimised power curve.

A. Turbulence Intensity based Jensen Model (TI-JM)

The TI-JM is based on the Jensen model [28]. Wind speed (u_x) on a wake affected downstream turbine with radius (r_0) at distance (x) can be found with equation (1) using the Jensen model. Coefficient of thrust of the wake producing turbine is given by (C_T). The standard Jensen model and TI-JM require a pre-determined initial (standard) value of wake decay coefficient (k) for free-stream conditions. The value of k depends upon hub heigh (z) and surface roughness length (z_0) as given in equation (2). In the standard Jensen model, k remains constant as ideal wind conditions are assumed [28]. In reality, wind flow inside the farm is affected by deep array effect and wake-added turbulence intensity, which also affect k [5].

The TI-JM takes wake-added turbulence intensity into account while estimating wind speed deficit. The value of k varies inside the farm as per the wake-added turbulence intensity as given in equation (3) [4], where (I_u) is the longitudinal component of turbulence intensity. For a two turbines case, the TI-JM performs exactly the same as the standard Jensen model as only the standard value ($k = 0.07$) [5] is used for wake estimation. For the whole wind farm, values of k up to 0.20 were used for wake estimation inside the wind farm as suggested in [4].

$$u_x = u_0 \left(1 - \left(\frac{1 - \sqrt{1 - C_T}}{\left(1 + \frac{kx}{r_0}\right)^2} \right) \right) \tag{1}$$

$$k = \frac{1}{2 \ln\left(\frac{z}{z_0}\right)} \tag{2}$$

$$I_u = \frac{1}{\ln\left(z/z_0\right)} \qquad k = \frac{I_u}{2} \tag{3}$$

VII. WINDPRO

WindPRO is one of the most widely used and industry standard software for design, development and assessment of wind energy projects [5]. WindPRO calculations in this study are based on the WAsP (Wind Atlas Program) method. The standard Jensen model available in WindPRO and given in equation (1) is used for predicting wake losses. The standard value of $k = 0.07$ for onshore wind farms [5] is used in simulations. This value of k is same as in the TI-JM for two turbines case as discussed in section VI-A. Hence there is no difference between WindPRO and the TI-JM in case of two turbines as both use the standard Jensen model.

VIII. SIMULATION BASED RESULTS AND ANALYSIS

This section presents results and analysis based on simulations. Hard control simulations using all the collected data, when SMV6 was curtailed, are presented in section VIII-A. Simulation results based on optimised control are presented in section VIII-B. While simulations based on hard control with filtered data are presented in VIII-C.

A. Hard Control Simulations based on All Collected Data

All the collected data (unfiltered) during the experiment (when SMV6 was hard-curtailed) was used to execute a WindPRO based simulation. The simulation predicted an average production increase of almost 3% in SMV5 in the $200^\circ \pm 20^\circ$ sector, as compared to normal operation. The weighted increase in each 10° bin is shown in Figure 6. The greatest increase (1.15%) is achieved in the $190^\circ - 200^\circ$ bin. This was the prevailing wind direction during this experiment as evident from Figure 3. SMV5 is almost completely shadowed by SMV6 wake in the $190^\circ - 200^\circ$ bin. Hence WindPRO predicted a higher gain for this bin. The smallest increase is in the bin $200^\circ - 210^\circ$ where SMV5 is under full wake affects of SMV6. The wind blew less frequently in this bin, in comparison to the other three bins (see Figure 3). The production gain in the other two bins (partial wake conditions) is almost the same.

If equal weight (for wind direction and speeds) is given to all the bins then the gain in production increases as the wake moves from partial to full wake conditions. These WindPRO simulations show that curtailment of SMV6 can produce a greater increase in SMV5 power production in full or near-full wake conditions.

WindPRO predicted a loss in the combined production of SMV6 and SMV5 when SMV6 is hard curtailed as shown in Figure 6. The loss in the combined production shows that the loss in SMV6 production due to curtailment is not compensated by gain in SMV5 production. The greatest loss in combined production is predicted in the $180^\circ - 190^\circ$ bin as SMV5 is under minimal wake effect of SMV6, as compared to the other three bins. The loss in combined production decreases as the wake moves from partial to full wake conditions. The lowest loss is in full wake conditions, in the $200^\circ - 210^\circ$ bin.

B. Optimised Control Simulations

This section presents the simulations based on optimised control strategy using all the collected data (unfiltered, when SMV6 was curtailed) during the experiment. Figure 6 shows the optimised increase in SMV5 production in all the four bins. Simulations predicted that no combined increase can be achieved by curtailing SMV6 in the $180^\circ - 190^\circ$ bin, as wake impact on SMV5 is minimal. SMV6 follows its standard power curve (operating greedily) in this $180^\circ - 190^\circ$ bin, resulting in maximum combined production. When the wake moves to near-full wake conditions in $190^\circ - 200^\circ$ bin, SMV5 benefits more from curtailment of SMV6. The maximum possible gain in combined production is 0.4% in

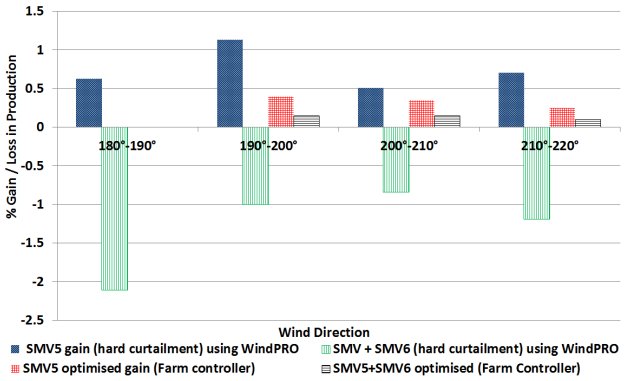

Fig. 6: Simulated % increase/decrease in SMV5 and combined production of SMV5+SMV6, using all the collected data

this bin $190° - 200°$, as wind conditions are favourable for implementation of coordinated control and wind blew more frequently in this bin.

The gain in production depends upon many parameters including number of turbines in the farm that can be curtailed and number of downstream turbines that can benefit from this curtailment, wind conditions and surface roughness on the site. The number of turbines that can be curtailed is only one. Turbulence intensity and roughness on the site is very high allowing the wake to diffuse quickly. Hence the optimised increase in SMV5 production and net gain is low. If all seven turbines in the farm are optimally controlled, a gain of up to 7% is possible in farm production in full or near-full wake conditions [4].

C. Hard Control Simulations based on Filtered Data

This section presents simulated results using the filtered data with the hard control strategy. These simulations are performed using the TI-JM and are presented in Table II. The impact of the curtailment strategy on downstream turbines and farm production in each valid data bin is analysed. The directional bins $180° - 190°, 190° - 200°$ and $210° - 220°$ are ignored as the number of data points in these bins are not significant. When the bin size is increased to $\pm 10°$, the number of valid data points are increased, fulfilling the filtering criteria. This results in some overlapping bins. Unfortunately, there are not enough valid data points available for Step 1 of the hard curtailment strategy. Filtering criteria given in section V is not met for Step 1. Hence results are only presented for Step 2. Valid speed bins range from 11m/s to 13m/s as data in only these speed bins fulfilled the filtering criteria.

SMV6 curtailment in the whole sector ($200° \pm 20°$) on average is 17.5% and in full wakes it is 18.6%. These simulations predict a decrease of up to 11% in combined production of SMV5 and SMV6, however an increase of up to 13% is predicted in SMV5 production. This indicates that SMV5 has benefited from the curtailment of SMV6. Impact of SMV6 hard curtailment on other turbines' and farm production is also shown in Table II. It should be noted that the combined production of SMV5 and SMV6 is different than simply adding the production of SMV5 and SMV6 given in Tables II and III. When combined production of the two turbines (SMV5 and SMV6) is analysed, the number of data points is increased, fulfilling the filtering criteria. When individual production of SMV5 or SMV6 is considered, number of data points is reduced and for some wind speed and direction bins, the filtering criteria was not met as explained earlier.

TABLE II: Simulated impact of SMV6 curtailment on SMV wind farm (% increase/decrease) using filtered data

Turbine(s)	$180° - 220°$	$190° - 210°$	$200° - 210°$	$200° - 220°$
SMV6	-17.5	-17.1	-18.6	-19
SMV5	4.0	13	12.5	-1.2
SMV4	4.2	4.0	-1.0	-1.0
SMV3	3.0	3.0	-1.0	-1.0
SMV2	2.0	2.0	-0.5	-0.5
SMV1	3.0	3.0	0	0
SMV5+SMV6	-9.5	-6.0	-6.0	-11
Farm	-2	-1.0	-2.5	-4.0

TABLE III: Actual impact of SMV6 curtailment on SMV wind farm (% increase/decrease) using filtered data

Turbine(s)	$180° - 220°$	$190° - 210°$	$200° - 210°$	$200° - 220°$
SMV6	-17.5	-17.1	-18.6	-19
SMV5	4.5	11.5	11.5	-0.7
SMV4	3.5	4.9	-0.9	-1.5
SMV3	2.0	2.3	-0.3	-0.5
SMV2	1.6	1.9	0.2	0.2
SMV1	2.6	2.7	0.5	0.6
SMV5+SMV6	-8.1	-5.6	-6.4	-10.9
Farm	-0.7	0.4	-1.9	-3.4

IX. Hard Control Field Results

Results in this section are based on filtered data obtained in this experiment, presented in Table III. These results are plotted with 80% confidence interval represented by the bar on the figures in this section. This confidence interval is chosen due to the limited data volume.

SMV6 power curve during the curtailment periods compared to the normal operations is shown in Figure 7. Average gain in SMV5 production is 4.5%. The highest gain in SMV5 production is observed in full wake conditions i.e. $200° - 210°$, which is 11.5%. The increase in SMV5 production confirms the positive impact of the hard curtailment strategy. The reduced wakes are propagated through the wind farm and increase in production is observed for all the downstream turbines SMV4–SMV1.

The combined production of SMV5 and SMV6 is decreased by almost 8.1% in the chosen directional sector. This means that the loss in SMV6 production is not compensated by gain in SMV5 production with the hard curtailment strategy.

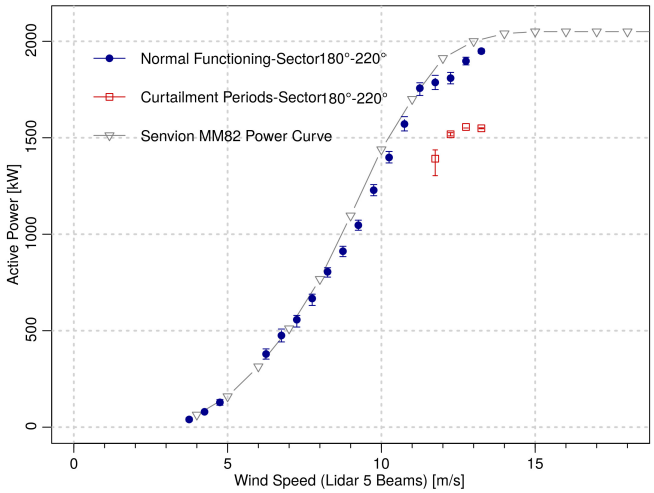

Fig. 7: SMV6 power curve obtained from data with 80% confidence interval

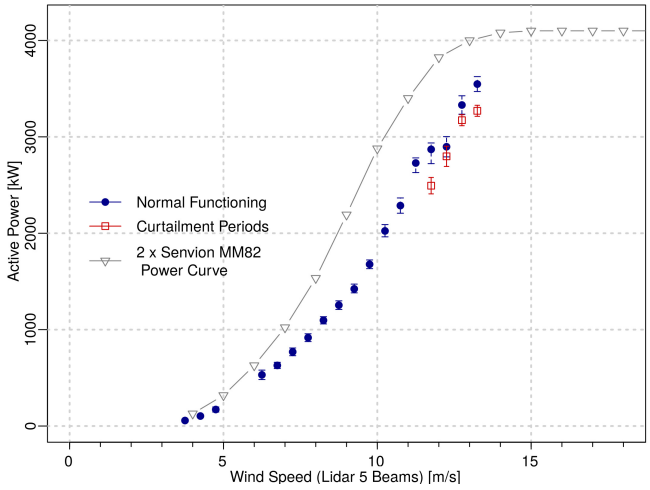

Fig. 8: Combined production of SMV5 + SMV6 in full wake ($200° - 210°$) conditions (80% confidence interval)

The lowest decrease in combined production is in full wake conditions as shown in Figure 8. By definition SMV6 wake has highest impact on SMV5 production in full-wake conditions. Hence, the benefits of curtailment are also greater in this bin. In partial wake conditions, impact of SMV6 is relatively low, hence gain in production due to curtailment, is also low.

This loss in combined production is the reason to opt for soft optimised control strategies. Simulations in section VIII-B suggest that when properly implemented, the optimised strategy never produces losses in combined production.

The farm production is reduced by an average of 0.7% as a result of SMV6 curtailment. The average farm production loss is less than 1%, indicating that the five downstream turbines have benefited from the 17.5% curtailment applied on SMV6. The farm power curve in the $200° \pm 20°$ is presented in Figure 9 showing the small loss in production during the curtailment period. This small decrease in overall farm production relative to normal operations suggests that if turbines are curtailed optimally then overall farm production can be increased.

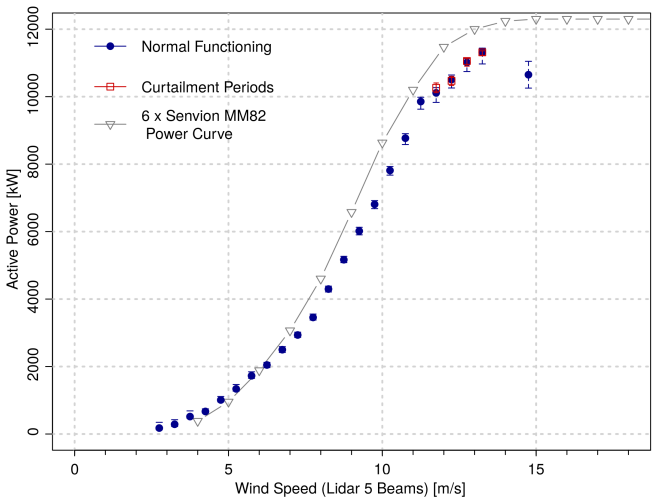

Fig. 9: Impact of the hard curtailment strategy on overall farm production in $200° \pm 20°$ bin (80% confidence interval)

Results in Table II can be compared with results in Table III. Simulations in section VIII-C predicted an overall increase of 4% in SMV5 production with the hard curtailment strategy (with filtered data) while an increase of 4.5% was observed in the actual experiment. Simulations predicted a decrease of 9.5% in combined production of SMV5 and SMV6, while the actual decrease is 8.1%. The overall decrease in farm production predicted with simulations is 2% while the actual decrease is 0.7%. A maximum difference of 1.5% is observed between simulated and real-time results. This shows that simulations are in good agreement with the field results.

X. Conclusion

Preliminary results of the C_P-based curtailment experiment from the SmartEOLE project are presented. The potential of coordinated control of wind farms, for increasing farm production, is investigated using live experiments. Two turbines in the SMV wind farm (SMV5 and SMV6) were chosen as the experiment turbines. The farm and turbines were equipped with modern LiDARs. SMV7 production was used as a reference for defining a two step hard curtailment strategy in the directional sector $200° \pm 20°$. The curtailment strategy reduced SMV6 production (using C_P) by a maximum of 20% for analysing the wake effect produced on SMV5 and the overall farm production.

Data from different sources was analysed during the curtailment period. WindPRO predicted 3% increase in SMV5 production with the given hard curtailment strategy in the chosen directional sector when all the collected data was simulated. A decrease in combined production of SMV5 and SMV6 was predicted as the loss in SMV6 production cannot be compensated by gain in SMV5 production. Optimised control strategy was simulated to predict the optimal power settings of SMV6. Simulations with the optimised strategy predicted an increase of up to 0.4% in SMV5 production.

A production increase of up to 11.5% was observed for the downstream turbine SMV5 with the field data. It was observed that the increase in SMV5 production becomes more

significant as the turbine moves from experiencing partial wake to full wake conditions. The gain in SMV5 production was propagated through the farm as the downstream turbines benefited from the reduced wake effects. Simulations performed with the TI-JM (using filtered data) has a difference of a maximum of 1.5% with the real time results, showing that simulations are in good agreement with field results.

A decrease in combined production of SMV5 and SMV6 and overall farm production (SMV1–SMV6) was observed with the hard curtailment strategy. This confirmed the importance of optimised control strategies. The simulations based on optimised strategy show that if SMV6 power is curtailed optimally, the loss in SMV6 power is always compensated by gain in SMV5 production. It should be noted that the only change required for implementing the optimised strategy is the control algorithm (greedy to optimised) and no additional hardware is required. The experimental setup given in section III-A was used only to obtain high frequency wind data. Offline optimisation can be a solution. But as observed in the SMV wind farm, atmospheric instability and abrupt changes in the wind characteristics require faster and computationally efficient on-line optimised control strategies.

It can be concluded that coordinated control of wind farms is beneficial for overall gain and production maximisation of downstream turbines. Wake affected turbine(s) can benefit from the curtailment of upstream turbine(s). Though a net increase in combined production was not observed in this experiment, the gain in SMV5 production proves that there is potential for coordinated control for maximising overall farm production. If turbines are curtailed optimally, this can increase the combined power production and hence the efficiency of a wind farm in certain wind conditions. The impact of coordinated control can be more significant in stable wind conditions such as offshore and dense wind farms as wakes travel for longer distances. If turbines are densely designed, more downstream turbines will be shadowed by upstream turbines' wakes, reducing farm production. If these wakes are controlled with an optimised strategy, a positive impact on overall farm production can be achieved.

ACKNOWLEDGEMENT

The authors would like to thank the French National Project SMARTEOLE (ANR-14-CE05-0034) and the Commonwealth Scholarships Commission UK.

REFERENCES

[1] J. A. Dahlberg, "Assessment of the Lillgrund windfarm: Power performance," Vatenfall, Vindkraft AB, Tech. Rep. 21858-1, September 2009.

[2] L. Y. Pao and K. E. Johnson, "A tutorial on the dynamics and control of wind turbines and wind farms," in *American Control Conference, ACC'09*. 172: IEEE, 2009, Conference Proceedings, pp. 2076–2089.

[3] F. A. Aranda, "Wind farm control methods, IEA R&D wind task 11 - topical expert meeting," International Energy Agency, Tech. Rep., November 2012.

[4] T. Ahmad, N. Girard, B. Kazemtabrizi, and P. Matthews, "Analysis of two onshore wind farms with a dynamic farm controller," in *EWEA, Paris France*, November 2015.

[5] N. Per, V. Jens, K. Jon, M. Per, J. Thomas, T. Morten, L., S. Mads, V., S. Thomas, S. Lasse, M. Mauricio, and B. Karina, *WindPRO 2.7 User Guide*, 3rd ed., EMD International A/S, Aalborg, Denmark, October 2010.

[6] E. Bitar and P. Seiler, "Coordinated control of a wind turbine array for power maximization," in *American Control Conference (ACC)*. 136: IEEE, 2013, Conference Proceedings, pp. 2898–2904.

[7] K. E. Johnson and N. Thomas, "Wind farm control: addressing the aerodynamic interaction among wind turbines," in *American Control Conference, ACC'09*. 155: IEEE, 2009, Conference Proceedings, pp. 2104–2109.

[8] G. Corten and P. Schaak, "Heat and flux: Increase of wind farm production by reduction of the axial induction," in *Proceedings of the European Wind Energy Conference*, 2003.

[9] C. Schram and P. Vyas, "Windpark turbine control system and method for wind condition estimation and performance optimization," Nov. 29 2005, US Patent App. 11/288,081.

[10] A. Ambekar, V. Ryali, and A. K. Tiwari, "Methods and systems for optimizing farm-level metrics in a wind farm," Dec. 1 2015, US Patent 9,201,410.

[11] J. Annoni, P. M. Gebraad, A. K. Scholbrock, P. A. Fleming, and J.-W. V. Wingerden, "Analysis of axial-induction-based wind plant control using an engineering and a high-order wind plant model," *Wind Energy*, vol. 19, pp. 1135–1150, 2015.

[12] P. Fleming, P. M. Gebraad, S. Lee, J.-W. Wingerden, K. Johnson, M. Churchfield, J. Michalakes, P. Spalart, and P. Moriarty, "Simulation comparison of wake mitigation control strategies for a two-turbine case," *Wind Energy*, vol. 18, no. 12, pp. 2135–2143, 2015.

[13] P. A. Fleming, P. M. Gebraad, S. Lee, J.-W. van Wingerden, K. Johnson, M. Churchfield, J. Michalakes, P. Spalart, and P. Moriarty, "Evaluating techniques for redirecting turbine wakes using SOWFA," *Renewable Energy*, vol. 70, pp. 211–218, 2014.

[14] M. Soleimanzadeh, R. Wisniewski, and S. Kanev, "An optimization framework for load and power distribution in wind farms," *Journal of Wind Engineering and Industrial Aerodynamics*, vol. 107, pp. 256–262, 2012.

[15] G. Corten, P. Schaak, and E. Bot, "More power and less loads in wind farms: Heat and Flux," in *European Wind Energy Conference & Exhibition, London, UK*, 2004.

[16] J. Schepers and S. Van der Pijl, "Improved modelling of wake aerodynamics and assessment of new farm control strategies," in *Journal of Physics: Conference Series*, vol. 75, no. 1. IOP Publishing, 2007.

[17] L. Machielse, S. Barth, E. Bot, H. Hendriks, and G. Schepers, "Evaluation of (Heat and Flux) farm control," ECN, Petten, The Netherlands, Tech. Rep. ECN-E–07-105, 2007.

[18] K. Boorsma, "Heat and flux. analysis of field measurements," ECN, Petten, The Netherlands, Tech. Rep. ECN-E–12-048, November 2012.

[19] S. Kanev and F. Savenije, "Active Wake Control: loads trends," ECN, Petten, The Netherlands, Tech. Rep. ECN-E–15-004, January 2015.

[20] J. Wagenaar, L. Machielse, and J. Schepers, "Controlling wind in ECN scaled wind farm," *Proc. Europe Premier Wind Energy Event*, pp. 685–694, April 2012.

[21] K. Boorsma, "Power and loads for wind turbines in yawed conditions," ECN-E-12-047, ECN, Petten, The Netherlands, Tech. Rep., 2012.

[22] T. Ahmad, P. Matthews, and B. Kazemtabrizi, "PSO based wind farm controller," in *The 11th edition of the International Conference on Evolutionary and Deterministic Methods for Design, Optimization and Control with Applications to Industrial and Societal Problems, EUROGEN-2015 Glasgow, UK*, September 2015, pp. 277–283.

[23] *Senvion MM82 [50 Hz/2050 kW] Product Description*, Senvion wind energy solutions, Senvion GmbH, Hamburg Germany, www.senvion.com/global/en/wind-energy-solutions/wind-turbines/mm/mm82/.

[24] O. Coupiac, "Four vertical extrapolation methods," *WindTech International*, vol. 12, no. 2, pp. 5–8, March 2016.

[25] S. Aubrun, D. Averbuch, S. Baleriola, C. Braud, M. Boquet, O. Coupiac, N. G. P. Devinant, F. Guillemin, E. Guilmineau, A. Leroy, D. Nelson-Grüel, D. Peaucelle, and A. Petit, "SMARTEOLE Deliverable D1-1: Installation Protocol and test plans for field test 1 and wind tunnel test 1 and 2," Maïa Eolis, Univ. Orléans, INSA-CVL, PRISME EA4229, IFPEN, LEOSPHERE, École Centrale de Nantes, LHEEA UMR CNRS 6598, LAAS-CNRS, Tech. Rep. ANR Project no 14-CE05-0034, September 2016, confidential.

[26] "Google earth," http://www.google.com/earth/ accessed 8 August 2017.

[27] M. M. Rienecker, M. J. Suarez, R. Gelaro, R. Todling, J. Bacmeister, E. Liu, M. G. Bosilovich, S. D. Schubert, L. Takacs, G.-K. Kim *et al.*, "MERRA: NASA's modern-era retrospective analysis for research and applications," *Journal of Climate*, vol. 24, no. 14, pp. 3624–3648, 2011.

[28] N. O. Jensen, "A note on wind generator interaction," Risø National Laboratory, Roskilde, Denmark, Tech. Rep. Risø -M-2411, November 1983.